

Symmetrical threshold model with independence on random graphs

Bartłomiej Nowak^{✉*} and Katarzyna Sznajd-Weron^{✉†}

Department of Theoretical Physics, Wrocław University of Science and Technology, Wrocław, Poland



(Received 28 February 2020; revised manuscript received 5 May 2020; accepted 7 May 2020; published 22 May 2020)

We study the homogeneous symmetrical threshold model with independence (noise) by pair approximation and Monte Carlo simulations on Erdős-Rényi and Watts-Strogatz graphs. The model is a modified version of the famous Granovetter's threshold model: with probability p a voter acts independently, i.e., takes randomly one of two states ± 1 ; with complementary probability $1 - p$, a voter takes a given state, if a sufficiently large fraction (above a given threshold r) of individuals in its neighborhood is in this state. We show that the character of the phase transition, induced by the noise parameter p , depends on the threshold r , as well as graph's parameters. For $r = 0.5$ only continuous phase transitions are observed, whereas for $r > 0.5$ discontinuous phase transitions also are possible. The hysteresis increases with the average degree $\langle k \rangle$ and the rewriting parameter β . On the other hand, the dependence between the width of the hysteresis and the threshold r is nonmonotonic. The value of r , for which the maximum hysteresis is observed, overlaps pretty well with the size of the majority used for the descriptive norms in order to manipulate people within social experiments. We put the results obtained within this paper into a broader picture and discuss them in the context of two other models of binary opinions: the majority-vote and the q -voter model. Finally, we discuss why the appearance of social hysteresis in models of opinion dynamics is desirable.

DOI: [10.1103/PhysRevE.101.052316](https://doi.org/10.1103/PhysRevE.101.052316)

I. INTRODUCTION

It is not surprising that binary opinion models are extremely popular among sociophysicists, given that the 1/2-spin Ising model is not only one of the most popular models of theoretical physics, but also absolutely fundamental for the theory of phase transitions. However, what is probably more surprising is that the binary-choice models have received considerably more theoretical attention than other choice models among social psychologists, sociologists, and economists [1,2]. One of the most important class of such models are the threshold models [3,4] taking root in the pioneering paper by Granovetter [5].

The idea behind these models is extremely simple—an agent takes state 1 (which can be interpreted as agree, adopt the innovation, join the riot, etc.) if a sufficiently large fraction (above a given threshold) of people in his or her neighborhood is in state 1. Originally the model was investigated under the assumption of perfect mixing (all-to-all interactions). However, in 2002 Watts adapted Granovetter's threshold model to a network framework [3]. We will use the same approach here, and therefore individuals will be influenced only by the nearest neighbors; i.e., interactions will take place only between agents that are directly linked.

There are two important differences between the Watts threshold model and other models of binary opinions, such as the Galam model [6–8], the majority-vote (MV) [9–20], the q -voter (qV) [21–28], or the threshold q -voter (TqV)

model [29–32]. The first difference, often considered the most important, is the heterogeneity—each agent is described by an individual threshold, and therefore some agents adopt a new state very easily, whereas others don't [3]. The second difference, which should be particularly important for physicists, is the lack of the up-down symmetry. Once an agent adopts a state 1 it cannot go back to the previous one. To make the threshold model comparable with other binary opinion models, we have introduced recently the homogeneous symmetrical threshold model [33]. Here we will call this model simply the symmetrical threshold (ST) model for brevity.

Previously we have studied two versions of the ST model, each with a different type of nonconformity (anticonformity or independence) on the complete graph [33]. Therefore we were able to obtain exact analytical results within the mean-field approach. Analogously as in other models of binary opinions, the introduction of nonconformity, whether in the form of anticonformity or in the form of independence, resulted in the appearance of the agreement-disagreement phase transitions. We have shown, that for the threshold $r = 0.5$, which corresponds to the majority-vote model, the phase transition is continuous, whereas for $r > 0.5$ discontinuous phase transitions appear within the model with independence. For the model with anticonformity, phase transitions are continuous for an arbitrary value of r . A similar phenomenon has been observed previously for the q -voter model—within the model with anticonformity, only continuous phase transitions are observed, whereas within the model with independence (known also as the nonlinear noisy voter model), discontinuous phase transitions appear for $q > 5$ [28,34,35].

In this paper we focus on the ST model with independence, because the hysteresis and tipping points, two signatures of

*bartlomiej.nowak@pwr.edu.pl

†katarzyna.weron@pwr.edu.pl

a discontinuous phase transitions, are common features of complex social systems [36–38]. We study the model on Erdős-Rényi (ER) and Watts-Strogatz (WS) graphs [39]. For the ER graph the pair approximation (PA) should give an accurate result, whereas the WS graph allows us to tune the structure from (1) the complete graph, for which the mean-field approximation (MFA) gives an exact result, through (2) random graphs for which the PA should work properly, to (3) small-world networks, which resemble the basic features of the real social networks. Because it has been shown recently that the size of the hysteresis may depend on the graph’s properties, we focus on this issue and check to what extend results found within the MV model and the qV model are universal [14,15,19,20,28,40].

II. MODEL

We consider a system of N individuals placed in the nodes of an arbitrary graph. Each node represents exactly one individual (interchangeably called *an agent, a spin, or a voter*). We consider a model of binary opinions, beliefs, and decisions, and thus each voter at time t is described by a binary dynamical variable $S_i(t) = \pm 1(\uparrow / \downarrow)$. At each elementary update Δt :

- (1) A site i is randomly chosen from the entire graph,
- (2) An agent at site i acts independently with probability p , i.e., changes its opinion to the opposite one $S_i(t + \Delta t) = -S_i(t)$ with probability $\frac{1}{2}$,
- (3) With complementary probability $1 - p$ it conforms to its k_i neighbors if the fraction of its neighbors in the same state is larger than r :
 - (a) $S_i(t + \Delta t) = 1$ if more than rk_i neighbors are in the state 1 or
 - (b) $S_i(t + \Delta t) = -1$ if more than rk_i neighbors are in the state -1 .

As usual, a single Monte Carlo step consists of N updates, $\Delta t = 1/N$, which means that one time unit corresponds to the mean update time of a single individual. Under the above algorithm the following changes are possible in the system:

$$\begin{aligned}
 & \underbrace{\uparrow\uparrow \dots \uparrow\uparrow}_{>[rk_i]} \downarrow \xrightarrow{1-p} \underbrace{\uparrow\uparrow \dots \uparrow\uparrow}_{>[rk_i]} \uparrow\uparrow, \\
 & \underbrace{\downarrow\downarrow \dots \downarrow\downarrow}_{>[rk_i]} \uparrow \xrightarrow{1-p} \underbrace{\downarrow\downarrow \dots \downarrow\downarrow}_{>[rk_i]} \downarrow, \\
 & \underbrace{\dots\dots\dots}_{\text{any}} \uparrow \xrightarrow{p/2} \underbrace{\dots\dots\dots}_{\text{any}} \downarrow, \\
 & \underbrace{\dots\dots\dots}_{\text{any}} \downarrow \xrightarrow{p/2} \underbrace{\dots\dots\dots}_{\text{any}} \uparrow,
 \end{aligned} \tag{1}$$

where \downarrow and \uparrow denote states of a target agent, and $[rk_i]$ is the floor function of rk_i . In any other situation, the state of the system does not change.

In the Watts threshold model flipping from \uparrow to \downarrow , was forbidden [3]. Therefore, the model was asymmetrical contrary to the majority vote or the q voter.

In the original threshold model an arbitrary value of $r \in [0, 1]$ is possible, which is a reasonable assumption for the asymmetrical model describing the adoption to the new state. In the symmetrical case, the situation for $r < 0.5$ is less obvious. It can be easily seen within the following example: let the threshold $r < 0.5$ and the neighborhood of a target voter consist of 50% positive and 50% negative agents. It means that both opinions (positive and negative) could be adopted by the voter. Which one should be chosen in such a situation?

There are several possibilities to solve the above ambiguity, e.g., we can assume that (1) a voter prefers to change opinion and therefore will always change it to the opposite one whenever possible [30,32], (2) a voter prefers to keep an old opinion—this assumption overlaps $r \geq 0.5$ [29,33], or (3) a voter makes a random decision to flip or keep an old state. Each of these scenarios can be used. However, for modeling opinion or belief formation the second one, $r \geq 0.5$, seems to be the most justified from the social point of view [31].

III. ANALYTICAL APPROACH WITHIN PAIR APPROXIMATION

Our analytical approach is based on the pair approximation (PA), an improved version of the standard mean-field approximation (MFA), which already has been applied to various binary-state dynamics on complex networks [28,32,41,42].

Because at each elementary update only one voter can change his or her opinion, thus the number of agents with positive opinion N_\uparrow increases or decreases by 1 or remains constant. As in Ref. [34] we denote by $c = N_\uparrow/N$ the concentration of the positive opinion, which in an elementary time step increases or decreases by $\frac{1}{N}$ or remains constant. We also denote transition probabilities as in Ref. [22]:

$$\begin{aligned}
 \gamma^+ &= \text{Prob} \left[c(t + \Delta t) = c(t) + \frac{1}{N} \right], \\
 \gamma^- &= \text{Prob} \left[c(t + \Delta t) = c(t) - \frac{1}{N} \right], \\
 \gamma^0 &= \text{Prob} [c(t + \Delta t) = c(t)] = 1 - \gamma^+ - \gamma^-.
 \end{aligned} \tag{2}$$

For $N \rightarrow \infty$ we can safely assume that random variable c localizes to the expectation value, and we get the following continuous-time dynamical system:

$$\frac{dc}{dt} = \gamma^+ - \gamma^-, \tag{3}$$

in the rescaled time units t . The simplest and the most popular approach under which formulas for transition probabilities γ^\pm can be derived analytically is the simple mean-field approximation [21–23,29–31,33]. It gives very good agreement for the complete graph, but rarely for more complicated structures, because it neglects all fluctuations in the system by assuming that the local concentration of spins up is equal to the global one.

Another method, which works particularly well for random graphs with low clustering coefficient, is the pair

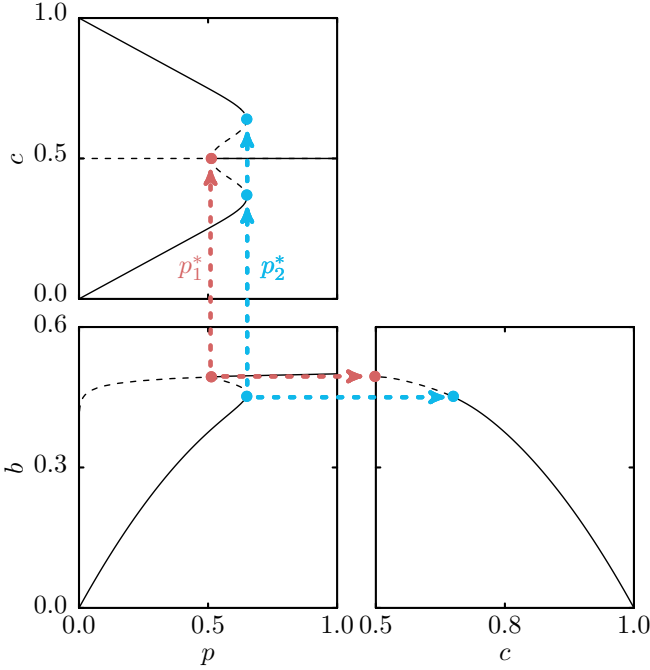


FIG. 1. Dependencies between the stationary value of the concentration of spins up c and active bonds b and the noise p obtained within the PA for sample values of parameters $\langle k \rangle = 80$ and $r = 0.6$. Results are presented in three phase-space projections: (c, p) , (b, p) , and (b, c) . For $p < p_1^*$ the only stable solution is the ordered phase, in which the symmetry between \uparrow and \downarrow states is broken, whereas for $p > p_2^*$ the only stable solution is the disordered phase.

approximation. Within the PA we describe the system by two differential equations—one for the time evolution of the concentration c of spins up and the second one for the time evolution of the concentration b of active bonds or links (bonds between two opposite spins) [2,28,41]:

$$\frac{dc}{dt} = - \sum_{j \in \{1, -1\}} c_j \sum_k P(k) \sum_{i=0}^k \binom{k}{i} \theta_j^i (1 - \theta_j)^{k-i} \times f(i, r, k, p) j, \quad (4)$$

$$\frac{db}{dt} = \frac{2}{\langle k \rangle} \sum_{j \in \{1, -1\}} c_j \sum_k P(k) \sum_{i=0}^k \binom{k}{i} \theta_j^i (1 - \theta_j)^{k-i} \times f(i, r, k, p) (k - 2i), \quad (5)$$

where c_j is the concentration of spins in state $j = \pm 1$ and thus $c_1 = c$, $c_{-1} = 1 - c$, $P(k)$ is the degree distribution of a graph and $\langle k \rangle$ is the average node degree. The parameter θ_j is the conditional probability of selecting a node that is in the opposite state to its neighbor in a state j , which is equivalent to the probability of choosing an active link from all links of a node in state j and can be approximated by [2,28]

$$\theta_j = \frac{b}{(2c_j)}, \quad (6)$$

where $f(i, r, k, p)$ is the flipping probability, i.e., the probability that a node in state j changes its state under the condition that exactly i from its k links are active.

Within our version of the threshold model, a voter flips with probability $1/2$ due to the independence, which takes place with probability p or due to the conformity, which takes place with probability $1 - p$ if more than $\lfloor rk \rfloor$ of its nearest neighbors are in the opposite state and thus

$$f(i, r, k, p) = \frac{p}{2} + (1 - p) \mathbb{1}_{\{i > \lfloor rk \rfloor\}}, \quad (7)$$

where $\mathbb{1}_{\{i > \lfloor rk \rfloor\}}$ is the indicator function, i.e. giving 1 for $i > \lfloor rk \rfloor$ and 0 otherwise.

In this paper, we focus mainly on the WS graph, because it allows us to tune the structure from the one with a high clustering coefficient and high average path length to the one with a low clustering coefficient and low average path length, by changing the parameter (rewiring probability) β without changing the average node degree $\langle k \rangle$. The degree probability $P(k)$ for such a network equals [43]

$$P(k) = \sum_{n=0}^{\min(k - \langle k \rangle / 2, \langle k \rangle / 2)} \binom{\langle k \rangle / 2}{n} (1 - \beta)^n \beta^{\langle k \rangle / 2 - n} \times \frac{(\beta \langle k \rangle / 2)^{k - \langle k \rangle / 2 - n}}{(k - \langle k \rangle / 2 - n)!} e^{-\beta \langle k \rangle / 2}. \quad (8)$$

The PA works properly for small clustering coefficients which correspond to large values of β . Moreover, under the assumption $\beta \rightarrow 1$, calculations simplify substantially, since Eq. (8) reduces to

$$P(k) = \frac{(\langle k \rangle / 2)^{k - \langle k \rangle / 2}}{(k - \langle k \rangle / 2)!} e^{-\langle k \rangle / 2}. \quad (9)$$

Therefore, we take in further calculations $P(k)$ given by Eq. (9), which is very close to the Poisson distribution centered at mean value $\langle k \rangle$ for the ER graph.

After inserting $f(i, r, k, p)$, given by Eq. (7), into Eqs. (4) and (5) we obtain

$$\frac{dc}{dt} = - \sum_{j \in \{1, -1\}} c_j \sum_k P(k) \times \left[\frac{jp}{2} + j(1 - p) \sum_{i=\lfloor rk \rfloor + 1}^k \binom{k}{i} \theta_j^i (1 - \theta_j)^{k-i} \right], \quad (10)$$

$$\frac{db}{dt} = \frac{2}{\langle k \rangle} \sum_{j \in \{1, -1\}} c_j \sum_k P(k) \left[pk \left(\frac{1}{2} - \theta_j \right) + (1 - p) \sum_{i=\lfloor rk \rfloor + 1}^k \binom{k}{i} \theta_j^i (1 - \theta_j)^{k-i} (k - 2i) \right]. \quad (11)$$

The steady states can be obtained by solving the following equations:

$$\frac{dc}{dt} = 0, \quad (12)$$

$$\frac{db}{dt} = 0. \quad (13)$$

Analogously as for the q -voter model with independence, we are not able to solve the above equations explicitly, but we can obtain inverse relation $p = p(c)$, instead of $c = c(p)$ [34]. For the concentration of active bonds we can present only an implicit solution.

One solution of Eq. (12), namely, $c = 1/2$, is straightforward because it is seen that for this value the right side of Eq. (10) equals zero, i.e., point $c = 1/2$ is the fixed point for all values of p . On the other hand, the right side of Eq. (11) is nonzero at $c = 1/2$ for arbitrary p ; thus from Eq. (13) for $c = 1/2$ we can derive the relation $p(b)$:

$$p = \frac{\sum_k P(k) \sum_{i=\lfloor rk \rfloor + 1}^k \binom{k}{i} b^i (1-b)^{k-i} (k-2i)}{-\langle k \rangle (\frac{1}{2} - b) + \sum_k P(k) \sum_{i=\lfloor rk \rfloor + 1}^k \binom{k}{i} b^i (1-b)^{k-i} (k-2i)}. \tag{14}$$

We see that $b \rightarrow 0$ gives $p = 0$ and $b \rightarrow 1/2$ gives $p = 1$.

To show the behavior of the system for $c \neq 1/2$ we insert Eq. (10) to Eq. (12), which allows us to derive the relation

$$p = \frac{\sum_k P(k) \sum_{i=\lfloor rk \rfloor + 1}^k \binom{k}{i} [c\theta_{\uparrow}^i (1-\theta_{\uparrow})^{k-i} - (1-c)\theta_{\downarrow}^i (1-\theta_{\downarrow})^{k-i}]}{\frac{1}{2} - c + \sum_k P(k) \sum_{i=\lfloor rk \rfloor + 1}^k \binom{k}{i} [c\theta_{\uparrow}^i (1-\theta_{\uparrow})^{k-i} - (1-c)\theta_{\downarrow}^i (1-\theta_{\downarrow})^{k-i}]}, \tag{15}$$

where we denote $\theta_{1/-1}$ by $\theta_{\uparrow/\downarrow}$ for clarity. Note that the above equation is in fact the relation $p = p(c, b)$, because both b and c are implicitly included in θ_{\uparrow} and θ_{\downarrow} according to Eq. (6). Thus, to solve the above equation we need the relation $b = b(c)$, which can be obtained by inserting the above equation into Eq. (13):

$$0 = \sum_k P(k) \sum_{i=\lfloor rk \rfloor + 1}^k \binom{k}{i} \{ c\theta_{\uparrow}^i \times (1-\theta_{\uparrow})^{k-i} [\langle k \rangle (1-2b) + (1-2c)(k-2i)] + (1-c)\theta_{\downarrow}^i (1-\theta_{\downarrow})^{k-i} [(1-2c)(k-2i) - \langle k \rangle (1-2b)] \} \tag{16}$$

As we have noticed above, Eq. (15) gives the relation $p = p(c, b)$, which can be plotted in three different planes, as shown in Fig. 1. There are two critical points, seen in this plot: (1) $p = p_1^*$, in which the solution $c = 1/2$ loses stability (so-called lower spinodal) and (2) $p = p_2^*$, in which the solution $c = c(p) \neq 1/2$, given by Eq. (15), loses stability. There are several possibilities to calculate $p = p_1^*$ [22,28,31]. Here we use method based on the observation that $p = p_1^*$ corresponds to the point $c = 1/2$ in the relation $b = b(c)$ (right bottom panel of Fig. 1). Therefore, first we take a limit $c \rightarrow 1/2$ in Eq. (16), which gives

$$0 = \sum_k P(k) \sum_{i=\lfloor rk \rfloor + 1}^k \binom{k}{i} b^i (1-b)^{k-i} \times \left[k - \langle k \rangle (1-2b) \left(1 + \frac{kb}{1-b} \right) - 2i + \langle k \rangle (1-2b) \left(1 + \frac{b}{1-b} \right) i \right]. \tag{17}$$

and then derive b from the above equation. Finally we insert this value of b into Eq. (14), which gives $p = p_1^*$. The upper

spinodal, i.e., point $p = p_2^*$, where $p = p(c)$ has two maxima (see Fig. 1), can be calculated numerically from Eq. (15) by taking a maximum value of p .

IV. DISCUSSION OF THE PAIR APPROXIMATION RESULTS

It was shown that for the majority-vote model with inertia there are two ingredients responsible for the discontinuous phase transitions: (1) the level of inertia and (2) the average node degree $\langle k \rangle$ [15,19]. Similarly, for the q -voter model (1) the size of the influence group q and (2) $\langle k \rangle$ are key factors influencing the type of the phase transition [28,34,40]. The question is if the same can be seen within the ST model.

The first ingredient influencing the phase transition is studies in the previous paper already within the mean-field approach [33]. We have observed continuous phase transitions for $r = 0.5$ and discontinuous ones for $r > 0.5$. We have obtained a similar result within the PA, as shown in Fig. 2: for small values of r we observe a continuous phase transition, whereas for large r a discontinuous one. This result is similar to results obtained within the MV model with inertia and the qV model. In both models discontinuous phase transitions were observed only for the sufficiently large value of inertia θ [15,19] or the large size of the influence group q [28,34]. It should be noticed that both the large size of the influence group q and the high threshold r correspond to the high value of inertia:

qV model: it is unlikely that we find a unanimous group of size q if q is large

ST model: it is unlikely that we find a fraction of agents in the same state larger than r if r is large.

Therefore, in both cases a voter is unlikely influenced by neighbors, i.e., its inertia is larger.

Now it is time to investigate the second ingredient, namely, to check whether $\langle k \rangle$ influences phase transitions within the ST model. In Fig. 3 we present the dependence between the

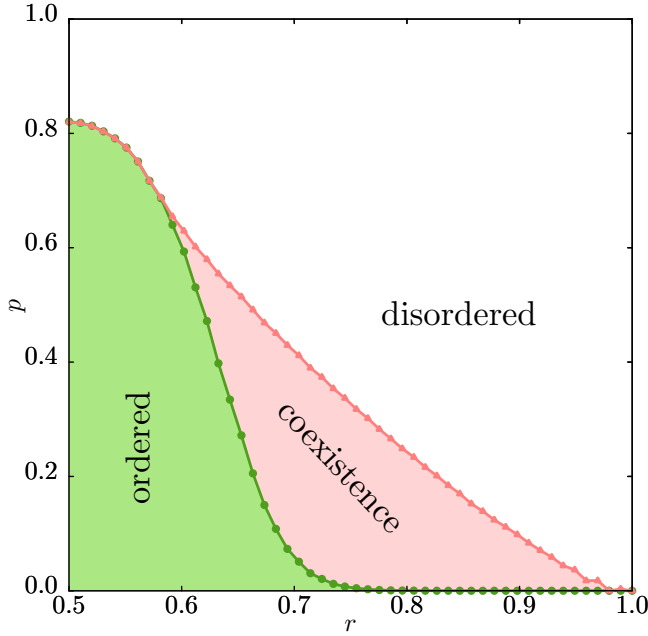


FIG. 2. Phase diagram for the average degree $\langle k \rangle = 50$. Lines with \bullet and \blacktriangle represent spinodals obtained within PA from Eqs. (15)–(17), i.e., limits of the region with metastability, in which the final state depends on the initial one.

stationary concentration of spins up c and the noise p for several values of the average node degree of the network $\langle k \rangle$ and two values of the threshold r . Again we see that for $r = 0.5$ only continuous phase transitions are observed independently of $\langle k \rangle$. However, for $r = 0.6$ the character of the phase transition changes with $\langle k \rangle$. Similarly as for the MV model with inertia and the qV model, the width of the hysteresis increases with $\langle k \rangle$ [15,19,40].

To the best of our knowledge, the dependence between the size of the hysteresis and $\langle k \rangle$ was not investigated precisely for the MV model with inertia. However, for the q -voter model it has been shown that $\langle k \rangle$ influences substantially the width of

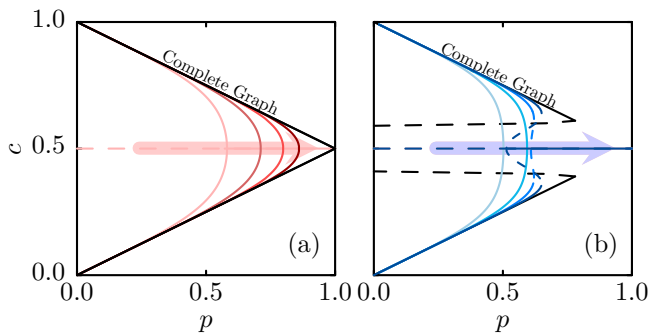


FIG. 3. Dependence between the stationary concentration of spins up c and the noise p for several values of the average node degree $\langle k \rangle$ and two values of the threshold: (a) $r = 0.5$ and (b) $r = 0.6$. Thin (red and blue colors online) lines refer to different values of $\langle k \rangle \in \{10, 20, 40, 80\}$ from left to right, whereas thick black lines represent the mean-field solution. Arrows indicate the direction in which $\langle k \rangle$ increases.

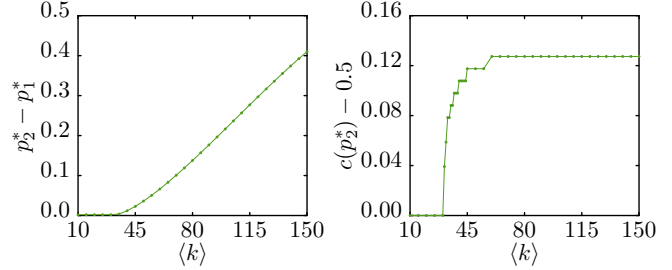


FIG. 4. The width of hysteresis $p_2^* - p_1^*$ (left panel) and the jump of the public opinion c (right panel) as a function of the average node degree $\langle k \rangle$ for threshold $r = 0.6$ obtained within PA.

the hysteresis and has almost no influence on the jump of the order parameter, defined as [40]

$$m = \frac{N_\uparrow - N_\downarrow}{N} = 2\frac{N_\uparrow}{N} - 1 = 2c - 1. \quad (18)$$

In this paper we did not introduce the order parameter m , because we made all calculations in terms of c . Of course, we could easily reformulate all results using the simple relation between m and c , given by Eq. (18).

In Ref. [40] the jump of m has been measured at upper spinodal. Therefore we also measure a jump of c at this point, i.e. $c(p_2^*) - 0.5$. As we see in Fig. 4 both hysteresis as well as the jump of c depend on $\langle k \rangle$. However, these dependencies are very different. There is only one common feature seen in both relations—below a certain value of $\langle k \rangle$ both $p_2^* - p_1^*$ as well as $c(p_2^*) - 0.5$ are equal zero, which indicates a continuous phase transition. Above this value the width of hysteresis increases almost linearly, for some intermediate values of $\langle k \rangle$, but then the growth significantly slows down and the hysteresis asymptotically approaches the limiting value, which is visible in Fig. 5. In result a hysteresis is an S-shaped curve, and the limiting value is given by mean-field size of the hysteresis [33]. On the other hand, the jump of concentration of spins up increases only slightly, but this growth is very rapid and takes place in a relatively small range of $\langle k \rangle$. For larger values of $\langle k \rangle$ the jump of c does not change, similarly as for the q -voter model [40].

Until now we have analyzed the influence of $\langle k \rangle$ on the phase transition only for $r = 0.6$. Of course, the same can be done for an arbitrary value of r , as shown in Fig. 5. We see that the width of the hysteresis indeed increases monotonically with $\langle k \rangle$. However, the dependence on the threshold r is much more interesting. There is an optimal value of r , which decreases with $\langle k \rangle$, for which the hysteresis has the maximum size.

Because empirical studies suggest that the mean number of friends varies typically from 5 to 150, depending on the rated emotional closeness between them [44], an optimal value of r is that for which the maximum size of hysteresis appear lies in (0.65,0.85). We find this result particularly interesting from the social point of view, which will be commented on in the Conclusions.

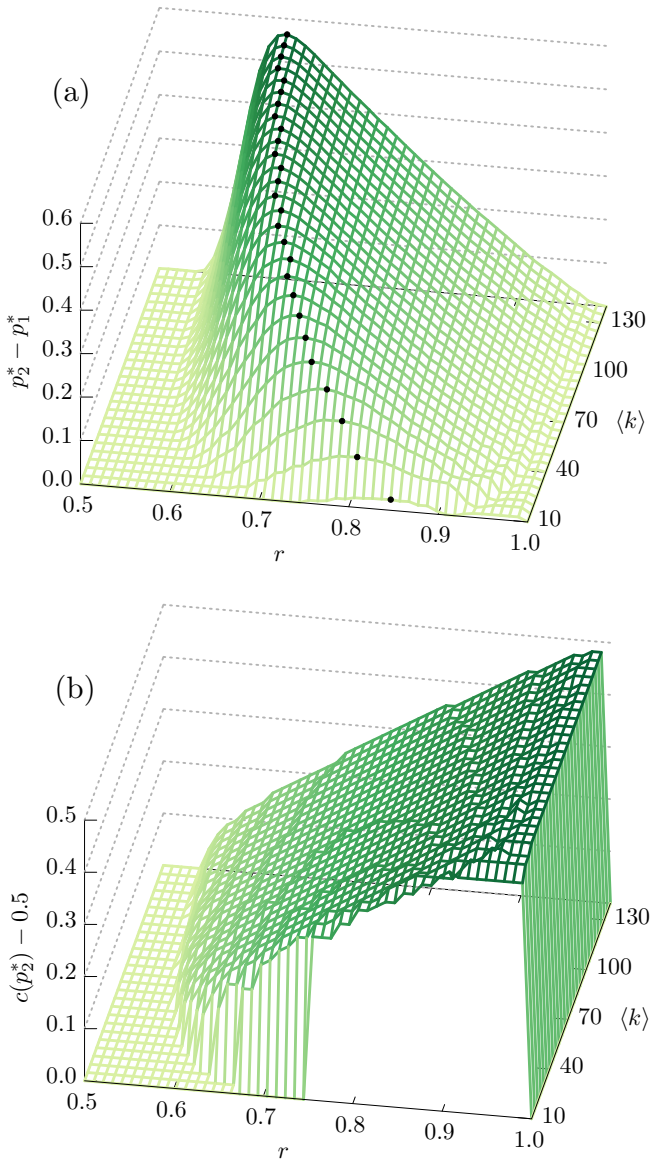


FIG. 5. The size of the hysteresis (a) and the jump of the concentration c at upper spinodal p_2^* (b) as a function of the threshold r and the average degree of a graph $\langle k \rangle$ obtained within the PA.

V. MONTE CARLO SIMULATIONS

We validate our analytical PA results with Monte Carlo (MC) simulations on ER and WS graphs [39]. We expect that the PA should give correct results for ER and WS graphs with $\beta = 1$. As we have observed in the Introduction, the WS algorithm allows us to tune the structure of the graph from a regular ($\beta = 0$) to a random one ($\beta = 1$). It also reduces to the complete graph for $\langle k \rangle = N - 1$. Moreover, in the whole spectrum of parameter β the average node degree is conserved. This makes the WS graph particularly interesting for our studies.

As expected, MC simulations for ER as well for WS graphs with $\beta = 1$ overlap the PA results, even for small values of $\langle k \rangle$; see Fig. 6. Moreover, this agreement is seen in all dependencies, namely, $c = c(p)$, $b = b(p)$, $b = b(c)$. The question is if and how the parameter β will influence results.

In Fig. 7 the parameter β varies from 0.1 to 1. The width of the hysteresis $p_2^* - p_1^*$ increases with β for $r > 0.5$ within the PA as well as MC simulations. To obtain the hysteresis from MC simulations we conduct simulations from two types of initial conditions: ordered ($c(0) = 1$) and disordered ($c(0) = 1/2$), as indicated in Fig. 7(a). As usual, in general the PA gives consistent results with MC simulations only for sufficiently large values of the rewiring probability β and big enough system size N , which is quite clear. First, within the PA we approximate all triangles, which are frequent in the case of high clustering coefficient, by pairs. Therefore, the higher clustering coefficient is (i.e., the lower β), the less accurate results are given by the PA. Second, PA equations are derived for the infinitely large system, and therefore the larger the system is, the better compatibility with the PA. Therefore to make a comparison with the PA we have chosen relatively large $N = 10^4$.

However, one may also ask how results scale with the system size. We have expected that our model will scale analogously to other binary models with up-down symmetry. Indeed, as shown in Fig. 8, critical exponents coincide with classical exponents for the Ising model, which have been also observed on various random networks [45], including Watts-Strogatz graphs [46]. Such a mean-field exponents have been also reported for various opinion dynamic models [47,48].

VI. CONCLUSIONS

The hysteresis and tipping points are common features of complex social and psychological systems [36,38,49–51]. For example, empirical studies suggest that public opinion exhibits both phenomena, which means that it remains seemingly resistant to change (which is related to hysteresis), and then a sudden, abrupt shift of opinion can be observed at the tipping point [36,38]. The notion of the tipping point, similar to the notion of the hysteresis, two signatures of discontinuous phase transitions, has been present in the social sciences for many years; for an early review of the importance of the notion of social hysteresis in social science see Ref. [50]. In the social sciences, the hysteresis is used to explain inelasticity of change and manifests as a slow response of societies to new problems, even if they are recognized by experts [36].

When it comes to the theoretical description of hysteresis in social science, different approaches are possible. One of the possibilities is Bourdieu's concept of the hysteresis effect [52], within which hysteresis is a consequence of interrelations between habitus (a property of actors, e.g., individuals, groups, or institutions) and field (social space); for a review see Ref. [53]. According to this concept, the hysteresis effect means that in the changed circumstances, individuals maintain their acquired dispositions, even when they are not suited to the new social context. Surprisingly, Bourdieu's concept is perfectly consistent with the idea of hysteresis appearing in the physics of phase transitions.

Although it may seem that the social hysteresis and the tipping point are just fancy buzzwords, empirical social studies have confirmed that they are not just abstract ideas [36,38,51].

These findings, among others, inspired researchers to look for the hysteresis in models of opinion dynamics [15,19,40]. For example, an additional noise has been introduced to the MV

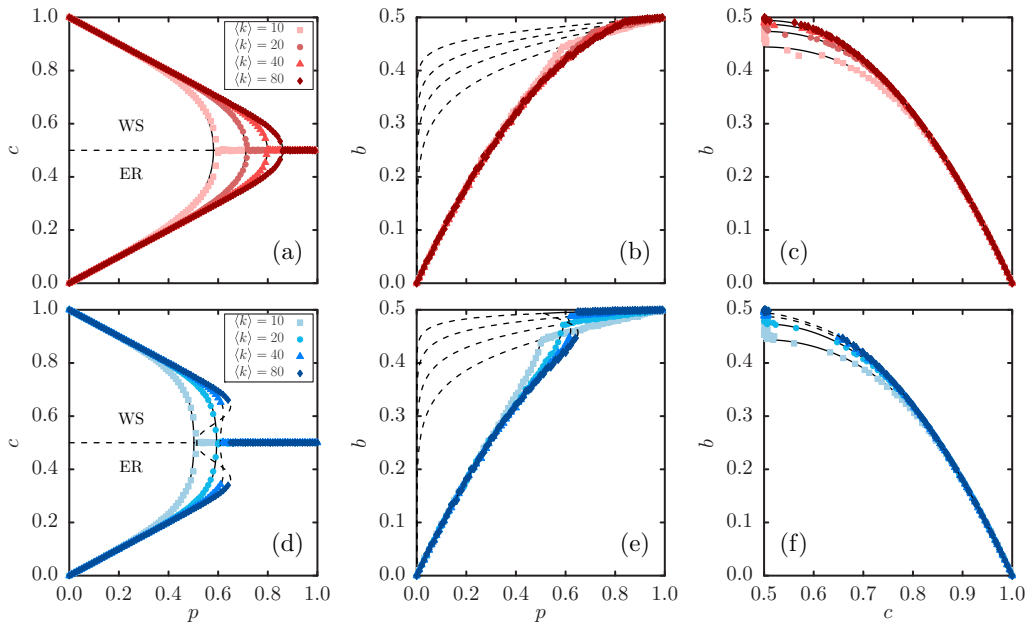


FIG. 6. Comparison between results obtained within the PA (denoted by lines) and Monte Carlo simulations (denoted by symbols) for $r = 0.5$ (upper panels) and $r = 0.6$ (bottom panels). In the left column [panels (a) and (d)] results for two types of graphs are presented: Watts-Strogatz with $\beta = 1$ [upper part, obtained from the initial condition $c(0) = 1$] and Erdős-Rényi [bottom part, obtained from the initial condition $c(0) = 0$]. In the remaining panels results for WS graphs with $\beta = 1$ are presented, but for ER graphs the results are the same. Solid lines correspond to stable, whereas dashed lines to unstable, solutions of Eqs. (12) and (13). For all diagrams the size of the system $N = 10^4$ and the thermalization time $t = 10^4$. Results are averaged only over five samples, but for this size of the system it is sufficient, as seen above.

model, but it was shown that it does not affect the type of the phase transition, and it remains continuous irrespective of the network degree and its distribution [14,20]. On the other hand it was shown that discontinuous phase transitions may appear in the MV model with inertia, when the inertia is above an appropriate level [15]. Later a question about the *fundamental ingredients for discontinuous phase transitions in the inertial majority vote model* was asked [19]. It was shown that low $\langle k \rangle$ leads to the suppression of the phase coexistence. A similar result has been also reported for the q -voter model [40].

This motivated us to check if the same behavior will be observed within the ST model introduced in Ref. [33]. We have shown, using PA and MC simulations, that indeed the type of the phase transition within ST model depends on threshold r , as well as the properties of the network $\langle k \rangle$ and β ; i.e., hysteresis increases with $\langle k \rangle$ and β . On the other hand, the dependence on r is nonmonotonic, which will be commented on below.

We discuss ST in the context of MV and q V models, because they have much in common, which has been already discussed in Ref. [33]. In particular, ST model with anticonformity is the generalization of the basic majority-vote model, which corresponds to $r = 0.5$. Moreover, the ST model with $r = 1$ reduces to the q -voter model on the random regular graph with degree q , i.e., if $\forall i k_i = k = q$. Finally, the ST model with an arbitrary value of r corresponds to the threshold q -voter model on the random regular graph with $\forall i k_i = k = q$ [29–32].

Moreover, as we have noticed in Sec. IV, the parameters that are mainly responsible for the discontinuous phase transitions, namely, the level of inertia θ in the MV model with inertia, the size of the influence group q in the q V model,

and the threshold r needed for the social influence in the ST model, play in a sense a similar role. The larger q or r is, the harder it is to influence a voter, which as a result increases inertia on the microscopic level.

Because the hysteresis can be viewed as an inertia of the system on the macroscopic level, it would not be surprising that the inertia on the microscopic level supports the hysteresis. However, as shown in Fig. 5, the relation between the size of the hysteresis and parameter r is not that trivial, i.e., it is nonmonotonic, having the maximum value for a given value of r , which depends on $\langle k \rangle$. This is a particularly interesting result from the social point view and worth discussions here.

It is known that social influence increases with the size of the influence group as well as the unanimity of the group. However, this dependence is far from being trivial. First, it increases only up to a certain level. The social influence is stronger if the group of influence consists of four, instead of two, people. However, above a certain threshold it remains on the same level. Moreover, above this threshold, around 7–11 people, the social influence decreases [54].

Therefore, in social experiments, in which descriptive norms are used to influence people, social psychologists use neither unanimity nor a simple majority. Instead they use a certain supermajority, often around 75%. For example, they manipulate people to reuse towels in hotels with the fake descriptive norm saying something like: “75% of our guests are reusing towels.” There is no strong evidence that 75% is the magic number, and in some other experiments larger majorities were used, as briefly reviewed in Ref. [31]. The main message we want to convey here is that the larger majority does not always result in stronger social influence. It seems that some optimal values exist, and these values probably

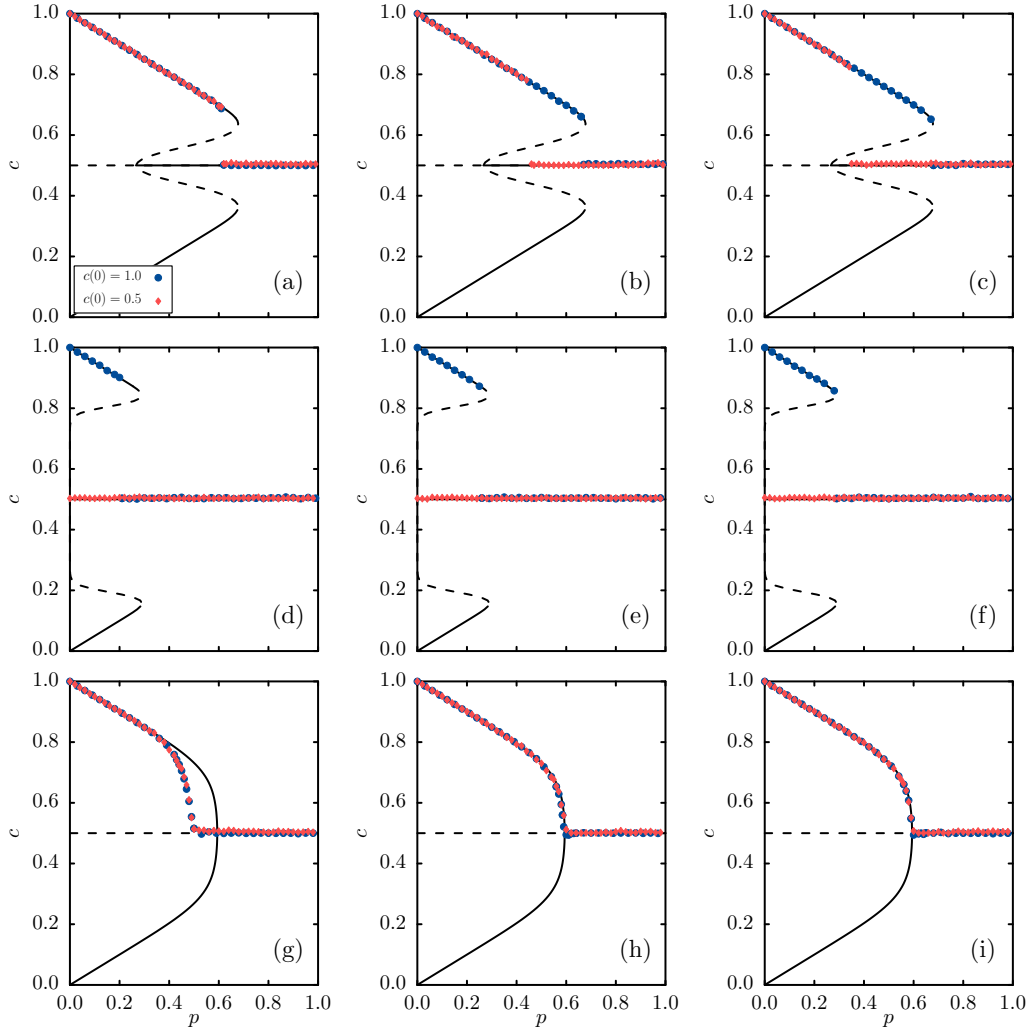


FIG. 7. Dependence between the stationary concentration of spins up c and the noise p for $r = 0.6$, $\langle k \rangle = 150$ (upper row), $r = 0.8$, $\langle k \rangle = 150$ (middle row), $r = 0.6$, $\langle k \rangle = 20$ (bottom row), and several values of the rewriting parameter: (a), (d), and (g) $\beta = 0.1$, (b), (e), and (h) $\beta = 0.5$, (c), (f), and (i) $\beta = 1$. Monte Carlo results for two types of initial conditions [as indicated in panel (a)] and $N = 10^4$ are denoted by symbols, whereas lines correspond to PA results. The thermalization time $t = 10^6$ for initial condition $c(0) = 0.5$ and $t = 2 \times 10^4$ for initial condition $c(0) = 1$. Results are averaged over five samples.

depend on the size of the influence group: for small groups unanimity is needed but for large groups some threshold value is more appropriate, significantly larger than 50%, but smaller than 100%. How is this related with the results obtained here?

As we have observed in Sec. IV, it was found empirically that in real social networks $\langle k \rangle \in (5, 150)$. This finding may seem surprising if we realize that, for example, on Facebook the current limit for the number of friends is 5000 people. Indeed, the growth of online communication raises a question about the scalability of the number of friends with the size of a social network. However, it seems that it is not a matter of the size of the whole social network that matters but rather the cognitive limits of our brain. As shown by Dunbar, the typical size of social groups correlates closely with the size of the neocortex. As a result *the structure of online social networks mirrors the offline network of face-to-face contacts and consists of layers at 5, 15, 50, and 150 individuals* [44]. For these values the optimal threshold of r , for which the largest social hysteresis is observed, lies in the range (0.65, 0.85), depending on the average size of the influence group $\langle k \rangle$. We admit

that what we measure is not the power of social influence, but the size of the hysteresis. However, having in mind that the hysteresis is usually observed in social systems, we can speculate that there are some optimal values in the level of social influence and these values influence the hysteresis that is usually observed in social systems.

We are aware that it maybe merely intriguing but the meaningless coincident. However, we believe that this finding deserves more attention and studies within other models of opinion dynamics.

Data sharing is not applicable to this article as no new data were created or analyzed in this study.

ACKNOWLEDGMENTS

This work is supported by funds from the National Science Centre (NCN, Poland) through Grant no. 2016/21/B/HS6/01256 and by PLGrid Infrastructure.

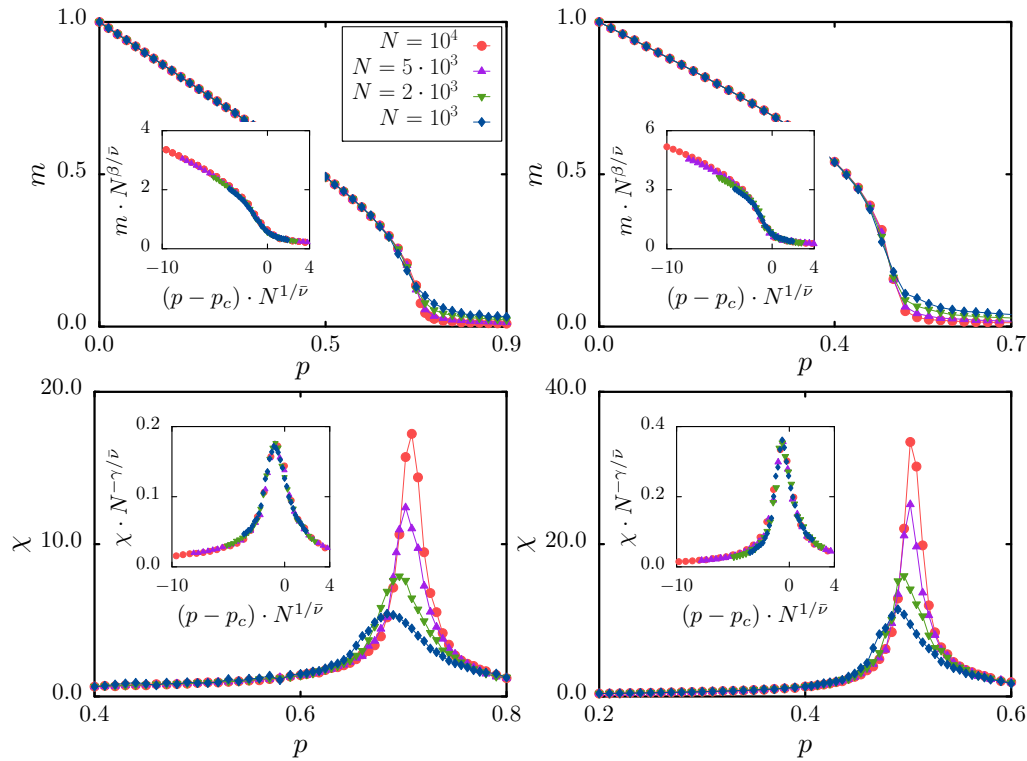


FIG. 8. Order parameter m (upper panels) and susceptibility χ (bottom panels) for $r = 0.5$, $\langle k \rangle = 20$ (left column), and $r = 0.6$, $\langle k \rangle = 10$ (right column) and different population sizes N , indicated in the left top panel. The corresponding scaling plots are shown in the respective insets. Presented data were obtained for $\beta \sim 1/2$, $\bar{\nu} \sim 2$, $\gamma \sim 1$, and $p_c \sim 0.714$ (left column) and $p_c \sim 0.512$ (right column).

- [1] D. Watts and P. Dodds, in *Threshold Models of Social Influence*, edited by P. Bearman and P. Hedström, (Oxford University Press, Oxford, 2017), pp. 475–497.
- [2] A. Jędrzejewski and K. Sznajd-Weron, *C. R. Phys.* **20**, 244 (2019).
- [3] D. J. Watts, *Proc. Nat. Acad. Sci. USA* **99**, 5766 (2002).
- [4] M. Grabisch and F. Li, *Dyn. Games Appl.* **10**, 444 (2019).
- [5] M. Granovetter, *Am. J. Sociol.* **83**, 489 (1978).
- [6] S. Galam, *J. Stat. Phys.* **61**, 943 (1990).
- [7] S. Galam, *Intl. J. Modern Phys. C* **19**, 409 (2008).
- [8] S. Galam, *Sociophysics: A Physicist's Modeling of Psycho-Political Phenomena* (Springer-Verlag, New York, 2012).
- [9] T. M. Liggett, *Interacting Particle Systems* (Springer, Berlin, 1985).
- [10] T. Tome, M. De Oliveira, and M. Santos, *J. Phys. A: Gen. Phys.* **24**, 3677 (1991).
- [11] M. de Oliveira, *J. Stat. Phys.* **66**, 273 (1992).
- [12] F. Lima and K. Malarz, *Intl. J. Mod. Phys. C* **17**, 1273 (2006).
- [13] J. Santos, F. Lima, and K. Malarz, *Physica A* **390**, 359 (2010).
- [14] A. Vieira and N. Crokidakis, *Physica A* **450**, 30 (2016).
- [15] H. Chen, C. Shen, H. Zhang, G. Li, Z. Hou, and J. Kurths, *Phys. Rev. E* **95**, 042304 (2017).
- [16] A. Fronczak and P. Fronczak, *Phys. Rev. E* **96**, 012304 (2017).
- [17] A. Krawiecki, *Eur. Phys. J. B* **91**, 50 (2018).
- [18] A. Krawiecki and T. Gradowski, *Acta Phys. Pol. B: Proc. Supp.* **12**, 91 (2019).
- [19] J. Encinas, P. Harunari, M. De Oliveira, and C. Fiore, *Sci. Rep.* **8**, 9338 (2018).
- [20] J. Encinas, H. Chen, M. de Oliveira, and C. Fiore, *Physica A* **516**, 563 (2019).
- [21] C. Castellano, M. A. Muñoz, and R. Pastor-Satorras, *Phys. Rev. E* **80**, 041129 (2009).
- [22] P. Nyczka, K. Sznajd-Weron, and J. Cisto, *Phys. Rev. E* **86**, 011105 (2012).
- [23] P. Moretti, S. Liu, C. Castellano, and R. Pastor-Satorras, *J. Stat. Phys.* **151**, 113 (2013).
- [24] M. Mobilia, *Phys. Rev. E* **92**, 012803 (2015).
- [25] M. A. Javarone and T. Squartini, *J. Stat. Mech.: Theory Exp.* (2015) P10002.
- [26] A. Mellor, M. Mobilia, and R. Zia, *Europhys. Lett.* **113**, 48001 (2016).
- [27] A. Mellor, M. Mobilia, and R. K. P. Zia, *Phys. Rev. E* **95**, 012104 (2017).
- [28] A. Jędrzejewski, *Phys. Rev. E* **95**, 012307 (2017).
- [29] P. Nyczka and K. Sznajd-Weron, *J. Stat. Phys.* **151**, 174 (2013).
- [30] A. R. Vieira and C. Anteneodo, *Phys. Rev. E* **97**, 052106 (2018).
- [31] P. Nyczka, K. Byrka, P. R. Nail, and K. Sznajd-Weron, *PLoS ONE* **13**, e0209620 (2018).
- [32] A. Vieira, A. F. Peralta, R. Toral, M. San Miguel, and C. Anteneodo, *arXiv:2002.04715v1* (2020).
- [33] B. Nowak and K. Sznajd-Weron, *Complexity* **2019**, 5150825 (2019).
- [34] P. Nyczka, J. Cisto, and K. Sznajd-Weron, *Physica A* **391**, 317 (2012).

- [35] A. Peralta, A. Carro, M. San Miguel, and T. R., *Chaos* **28**, 075516 (2018).
- [36] M. Scheffer, F. Westley, and W. Brock, *Ecosystems* **6**, 493 (2003).
- [37] R. Vallacher, S. Read, and A. Nowak (Eds.), *Computational Social Psychology* (Routledge Taylor & Francis Group, New York, 2017).
- [38] D. Centola, J. Becker, D. Brackbill, and A. Baronchelli, *Science* **360**, 1116 (2018).
- [39] D. J. Watts and S. H. Strogatz, *Nature (London)* **393**, 440 (1998).
- [40] A. Abramiuk and K. Sznajd-Weron, *Entropy* **22**, 120 (2020).
- [41] J. P. Gleeson, *Phys. Rev. X* **3**, 021004 (2013).
- [42] A. Peralta, A. Carro, M. San Miguel, and R. Toral, *New J. Phys.* **20**, 103045 (2018).
- [43] A. Barrat and M. Weigt, *Eur. Phys. J. B* **13**, 547 (2000).
- [44] R. Dunbar, V. Arnaboldi, M. Conti, and A. Passarella, *Soc. Netw.* **43**, 39 (2015).
- [45] H. Hong, M. Ha, and H. Park, *Phys. Rev. Lett.* **98**, 258701 (2007).
- [46] H. Hong, B. Kim, and M. Choi, *Phys. Rev. E* **66**, 018101 (2002).
- [47] R. Toral and C. Tessone, *Commun. Comput. Phys.* **2**, 177 (2007).
- [48] N. Crokidakis and C. Anteneodo, *Phys. Rev. E* **86**, 061127 (2012).
- [49] E. Wolf, *J. Am. Plan. Assoc.* **29**, 217 (1963).
- [50] J. Elster, *Synthese* **33**, 371 (1976).
- [51] G. Doering, I. Scharf, H. Moeller, and J. Pruitt, *Nat. Ecol. Evol.* **2**, 1298 (2018).
- [52] P. Bourdieu, *The Logic of Practice* (Stanford University Press, Stanford, CA, 1990).
- [53] C. Hardy, *Pierre Bourdieu: Key Concepts* (Routledge Taylor & Francis Group, New York, 2012), p. 126–145.
- [54] S. E. Asch, *Sci. Am.* **193**, 31 (1955).